ELSEVIER

Chemical Geology 169 (2000) 383–397

CHEMICAL GEOLOGY
INCLUDING
ISOTOPE GEOSCIENCE

www.elsevier.com/locate/chemgeo

Geochemical and biological aspects of sulfide mineral dissolution: lessons from Iron Mountain, California

Katrina J. Edwards [a,b,*], Philip L. Bond [a], Greg K. Druschel [a], Molly M. McGuire [c], Robert J. Hamers [c], Jillian F. Banfield [a]

[a] *Department of Marine Chemistry and Geochemistry, McLean Lab, Mail Stop No. 8, Woods Hole Oceanographic Institution, Falmouth, MA 02543, USA*

[b] *University of Wisconsin-Madison, Department of Geology and Geophysics, 1215 W. Dayton St., Madison, WI 53706, USA*

[c] *University of Wisconsin-Madison, Department of Chemistry, 1101 University Avenue, Madison, WI 53706, USA*

Received 21 July 1999; accepted 3 January 2000

Abstract

The oxidative dissolution of sulfide minerals leading to acid mine drainage (AMD) involves a complex interplay between microorganisms, solutions, and mineral surfaces. Consequently, models that link molecular level reactions and the microbial communities that mediate them to field scale processes are few. Here we provide a mini-review of laboratory and field-based studies concerning the chemical, microbial, and kinetic aspects of sulfide mineral dissolution and generation of AMD at the Richmond ore body at Iron Mountain, California.

Keywords: Acid mine drainage; Pyrite; Sulfide dissolution; Microorganisms

1. Site description

Iron Mountain is considered as one of the most unique acid mine drainage (AMD) sites because of the extremely acidic, metal-rich waters encountered there. Iron Mountain is a massive sulfide ore body within rhyolitic host rock, located in the West Shasta Mining District of Northern California (Fig. 1). The ore body was mined between the 1860s and the 1960s for Ag, Au, Cu, Fe, Zn, and pyrite (for sulfuric acid). Prior to the late 1980s, when Superfund monies were used to construct a waste treatment facility that is still in use today, the drainage from Iron Mountain flowed without treatment into the Sacramento river, with deleterious environmental consequences such as massive fish kills. Currently, waste is diverted from disused subsurface mines to the treatment facility for neutralization of acidity and precipitation of metals.

A number of mines (Richmond, Hornet, Lawson, and others) generate acidic waters at Iron Mountain. However, the effluent from the Richmond mine tunnels (Fig. 1) is the most metal-rich (up to 200 g l^{-1}) and acidic (down to pH = −3.5) reported anywhere in the world (Alpers et al., 1994; Nordstrom, 2000). Hence, a great deal of research and environmental monitoring has focused on the Richmond ore body, tunnel system, and effluent. A compilation of the

* Corresponding author. Tel.: +1-508-289-3620.
E-mail address: kedwards@whoi.edu (K.J. Edwards).

0009-2541/00/$ - see front matter
PII: S0009-2541(00)00216-3

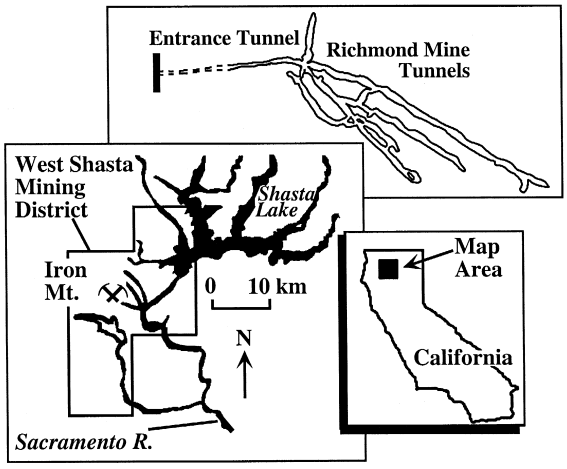

Fig. 1. Location maps of Iron Mountain, California, with a schematic plan-view layout of the Richmond Mine Tunnels.

Richmond effluent composition from 1940 to 1991 is available from the USGS (Alpers et al., 1992). The average flux of AMD from the Richmond Mine indicates that approximately 20 million moles of pyrite are oxidized every year (Nordstrom and Alpers, 1999a). At this rate, it will take ~3200 years for the pyrite at the Richmond ore body to oxidize (Nordstrom and Alpers, 1999a). Pyrite oxidation is highly exothermic, which is implied to account for the elevated temperatures at the Richmond, up to 50°C, particularly during heavy seasonal rainfalls (Edwards et al., 1999a).

Subsurface AMD sites, Iron Mountain among many others, are often inaccessible because of the hazardous conditions that result from frequent cave-ins. Consequently, the geochemistry and microbiology of AMD run-off streams in the vicinity of ore bodies are far better studied than subsurface sites in contact with ore bodies, and this is reflected in the available literature concerning AMD. In the 1980s, following a period of more than 35 years of unsafe conditions at Iron Mountain, renovations allowed access to the subsurface environments at the Richmond Mine. Site access for scientific studies at limited sites within Richmond Mine has been maintained since that time through regular renovations and maintenance. It is not known if the conditions at Iron Mountain are expressly unique, or if access to subsurface sites of primary acid generation (i.e., in contact with acid-generating ore bodies) is what sets Iron Mountain apart from other AMD systems. Further studies are required to determine if the conditions at Iron Mountain are truly unique, or if the site represents perhaps a rare opportunity to study processes that occur at other, inaccessible subsurface AMD sites.

2. AMD formation: reactions and products of sulfide dissolution

AMD is caused by the oxidative dissolution of sulfide minerals that have been exposed to surface air, water, and microorganisms. It is important to note that acid waters can occur in the absence of mining, and have historically been recognized (Nordstrom and Alpers, 1999b). Mining, however, frequently results in increased exposure of reactive mineral surfaces to oxidants. This has occurred at Iron Mountain due to the extensive tunnel systems and fracturing of the overall ore body.

Pyrite (FeS_2) is the most abundant sulfide on the Earth's surface. Consequently, kinetic aspects of pyrite oxidation have been studied more extensively than any other sulfide mineral (Williamson and Rimstidt, 1994; Rimstidt and Newcomb, 1992; Brown and Jurinak, 1989; Moses et al., 1987; McKibben and Barnes, 1986; Wiersma and Rimstidt, 1984; Garrels and Thompson, 1960; Stokes, 1901). Previous reviews of the pyrite oxidation literature have been made by Lowson (1982) and Nordstrom (1982), and more recently by Nordstrom and Southham (1997), and Nordstrom and Alpers (1999b).

At low pH, the rate of oxidative dissolution is controlled by the concentration of ferric iron, which interacts with reactive surface sites more effectively than oxygen (McKibben and Barnes, 1986). The overall stoichiometry of the reaction is commonly written as:

$$FeS_{2(s)} + 14Fe^{3+}_{(aq)} + 8H_2O_{(l)} \rightarrow 15Fe^{2+}_{(aq)} + 2SO^{2-}_{4(aq)} + 16H^{+}. \quad (1)$$

The rate-limiting step in the oxidative dissolution of pyrite is considered to be the oxidation of ferrous iron to regenerate ferric iron (Singer and Stumm, 1970).

Reaction (1) describes the overall stoichiometry of oxidative dissolution reactions, but it does not describe the individual steps that must occur in the oxidation of sulfide to sulfate because of the large number of electrons that is transferred. Intermediate species such as elemental sulfur, sulfoxy compounds, and sulfites may play an extremely important role in the overall reaction kinetics (Nordstrom and Southham, 1997).

The most widely accepted model of sulfide mineral dissolution was proposed by Singer and Stumm (1968). This model describes the sequential oxidation of surface sulfur atoms to form the thiosulfate anion, which is then liberated (along with Fe^{2+}) into solution. The thiosulfate anion is subsequently oxidized to sulfate. In this case the overall reaction (1) can be separated into the surface reaction (2) and solution phase reaction (3):

$$FeS_2 + 6Fe^{3+} + 3H_2O \rightarrow S_2O_3^{2-} + 7Fe^{2+} + 6H^+, \quad (2)$$

$$S_2O_3^{2-} + 8Fe^{3+} + 5H_2O \rightarrow 2SO_4^{2-} + 8Fe^{2+} + 10H^+. \quad (3)$$

An important aspect of this model is that it predicts the formation of only water-soluble products. However, numerous reports have shown that elemental sulfur also forms at surfaces (McGuire et al., 1999, in review; Sasaki et al., 1995; see below). A complete model of pyrite dissolution must incorporate the formation of all observed surface products.

2.1. Intermediate dissolution products on sulfide mineral surfaces

Chemical changes taking place on the mineral surface are important in at least two respects. Formation of secondary minerals at the surface has the potential for forming inert layers that might inhibit diffusion of oxidants to the surface, thereby slowing dissolution. Additionally, intermediate sulfur products that develop on surfaces can be used as an energy source for some microorganisms. The speciation of intermediates surface products and the kinetics of their production are crucial for understanding how they, and the microbial communities they support, impact overall sulfide dissolution rates.

Raman and X-ray photoelectron spectroscopy (XPS) have recently become quite commonly utilized techniques for the determination of chemical speciation at the surfaces of pyrite and other metal sulfides. Since elemental sulfur has no electronic dipole (and therefore no infrared absorption), Raman is a particularly good probe of elemental sulfur. To better understand the role of microorganisms in altering surface chemistry during dissolution, we have used Raman spectroscopy to analyze surfaces reacted in the laboratory with enrichment cultures of microorganisms known to be important members of the microbial community at the Richmond Mine (Edwards et al., 1997, 1998, 1999b). The enrichment culture contained the iron-oxidizing species, *Ferroplasma acidarmanus* and *Leptospirillum ferrooxidans*, as well as a sulfur oxidizer, *Thiobacillus caldus*. Pyrite was reacted with enrichment cultures under conditions within the ranges observed at Iron Mountain (pH 1.5 and 37°C). Fig. 2 shows a comparison of the Raman spectrum of a pyrite single crystal exposed to the enrichment culture (Fig. 2C) and the spectrum of a sample reacted abiotically in acid for the same length of time. The original starting surface (Fig. 2A) shows three primary peaks, 342, 377, and 435 cm^{-1}, that arise from bulk pyrite. After reaction for 22 days in acid, the surface shows little change in

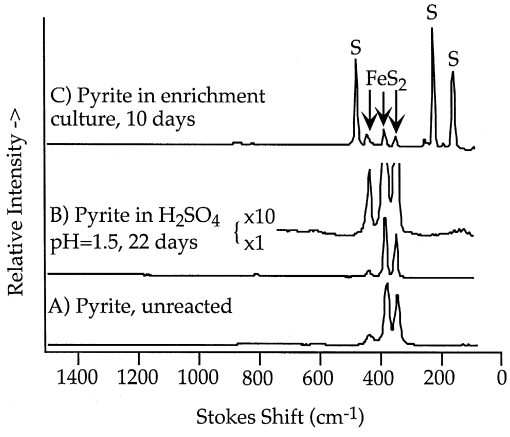

Fig. 2. Raman spectra of pyrite crystals. (A) Unreacted; (B) abiotically reacted with sulfuric acid, pH 1.5 for 22 days; (C) reacted with a mixed enrichment culture of iron- and sulfur-oxidizing microorganisms for 22 days (modified after McGuire et al., 1999, in review).

overall surface chemical composition, even when the scale is expanded by a factor of 10. However, in the presence of iron-oxidizing microorganisms, which can rapidly regenerate Fe^{3+}, the surfaces develop rather extensive sulfur layers. In this case, the Raman spectrum contains three very large, intense peaks at 470, 217, and 151 cm^{-1} that are characteristic of elemental sulfur, primarily in the form of S_8 rings. Calibration of the Raman data indicates that the sulfur layer is at least several hundreds of Angstroms thick if distributed uniformly over the mineral surface (McGuire et al., 1999, in review).

The formation of sulfur must arise from a different mechanism than the original Stumm model. For example, one possibility is direct attack on a sulfur site by a hydronium ion (H^+), via a mechanism such as:

$$MS + Fe^{3+} + H^+ \rightarrow M^{2+} + 1/2H_2S_n + Fe^{2+}, \quad (4)$$

$$1/2H_2S_n + Fe^{3+} \rightarrow 1/8S_8 + Fe^{2+} + H^+. \quad (5)$$

If the reaction of pyrite to sulfur is dominant, and sulfur accumulations do not limit surface oxidation rates, then the reaction of pyrite could be written as:

$$FeS_{2(S)} + 2Fe^{3+} \rightarrow 2S^0 + 3Fe^{2+}. \quad (6)$$

In this case, 1 mol of pyrite oxidation consumes only 2 mol of Fe^{3+}, compared to 14 in reaction (1). This is important, because the rate of pyrite oxidation is rate-limited by ferric iron supply. Also notable from reaction (6) is the absence of hydrogen ion release to solution, compared with 16 hydrogen ions released in reaction (1), emphasizing that the acid is generated from the oxidation of sulfur, for example:

$$S^0 + 1.5O_2 + H_2O \rightarrow SO_4^{2-} + 2H^+. \quad (7)$$

(Bahatti et al., 1993). Further studies are needed to quantify the formation of sulfur during pyrite oxidation in order to determine if the oxidation of elemental sulfur involves important, rate-limiting (in terms of acid generation) reactions.

Fig. 3 shows dissolution rate data, as indicated by the total iron concentration in solution over time, for pyrite reacted with the enrichment culture and reacted abiotically in acid. The difference in dissolution rate between these is approximately a factor of 2 (McGuire et al., 1999, in review). If the rate of sulfur formation correlates linearly with the dissolution rate,

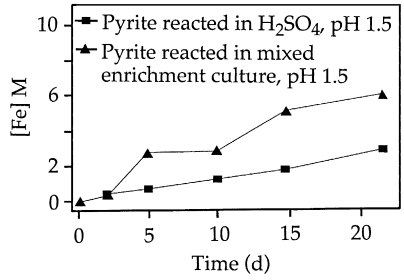

Fig. 3. Dissolution data for pyrite. Data for total iron release are shown for pyrite reacted abiotically in sulfuric acid, pH 1.5, and reacted in the presence of a mixed enrichment culture of iron- and sulfur-oxidizing microorganisms, also at pH 1.5 (modified after McGuire et al., in review).

a twofold difference in sulfur accumulation between the two samples is the maximum that would be expected because some sulfur will be consumed by the sulfur oxidizers in the enrichment culture. However, the Raman measurements on pyrite indicate that in the abiotic experiment, there is no detectable sulfur, while the microbial sample shows sulfur peaks that exceed those of the bulk pyrite by at least a factor of 10 (Fig. 2). Based on the signal-to-noise level of these measurements, the amount of sulfur on the abiotic sample is at least a factor of 100 less than that in the microbial experiment. The observation of a 100-fold difference in surface sulfur concentrations on samples whose nascent dissolution rates are different by a factor of 2 suggests that there may be an activation energy barrier to the formation of elemental sulfur at the surface.

2.2. Sulfur removal and reaction kinetics

Determining intermediate reactions involved in pyrite oxidation is critical because the overall reaction rate will be limited by the slowest kinetic step. If secondary phases such as sulfur form and inhibit diffusion to the surface, then at long times the overall dissolution rate will be controlled by the rate of oxidation of the surface product, rather than the rate of oxidation of the metal sulfide mineral itself. In the case of pyrite discussed above, quantitative analysis of the sulfur layer indicates that it is hundreds of Angstroms in thickness if distributed uniformly across the surface.

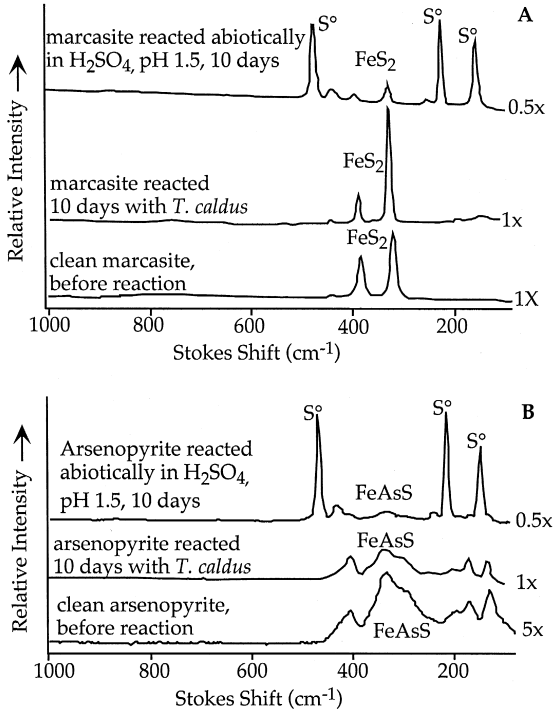

Fig. 4. Raman spectra for marcasite (A) and arsenopyrite (B). Data for surface composition are shown for unreacted samples, samples reacted with the sulfur-oxidizing bacterium *T. caldus*, and for samples reacted abiotically in sulfuric acid (pH 1.5; modified after McGuire et al., in review).

Many recent studies have suggested that the removal of sulfur by sulfur-oxidizing species in mixed consortia with iron oxidizers accounts for the higher dissolution rate of sulfide minerals in the presence of a mixed culture of S- and Fe-oxidizers as compared to a pure culture of only Fe-oxidizers (Dopson and Lindstrom, 1999; Curutchet et al., 1996; Garcia et al., 1995a,b). Another study demonstrated that sulfur removal increases dissolution rates at high concentrations of ferrous ions, also implying that accumulations may act as a diffusional barrier (Fowler and Crundwell, 1999). However, few studies have attempted to demonstrate that sulfur removal by sulfur-oxidizing microorganisms increases dissolution rates in the absence of iron-oxidizing bacterial catalysts.

A study of the effects of a sulfur-oxidizing isolate on sulfide mineral dissolution rate and surface sulfur accumulation revealed that the action of sulfur oxidizers alone does not increase dissolution rates, although it does lead to significant changes in surface composition (McGuire et al., 1999, in review). Fig. 4 shows Raman spectra of unreacted marcasite and arsenopyrite surfaces, as well as samples that were reacted in acid and that were exposed to a sulfur oxidizer isolated from Iron Mountain (*T. caldus*). In contrast to the Raman data for pyrite (Fig. 2), extensive sulfur formation is evident in the spectra for the marcasite and arsenopyrite samples that were abiotically reacted. When these minerals were exposed to the sulfur oxidizer, however, very little elemental sulfur was detectable. Fig. 5 shows the dissolution rate data for these same experiments. Note first that these minerals released more iron to the solution than pyrite (Fig. 3), indicating a higher reactivity, which in part accounts for the differences in sulfur accumulation on marcasite and arsenopyrite compared with abiotically reacted pyrite. Also note that dissolution rates are not increased in the presence of sulfur-oxidizing microorganisms, which we know

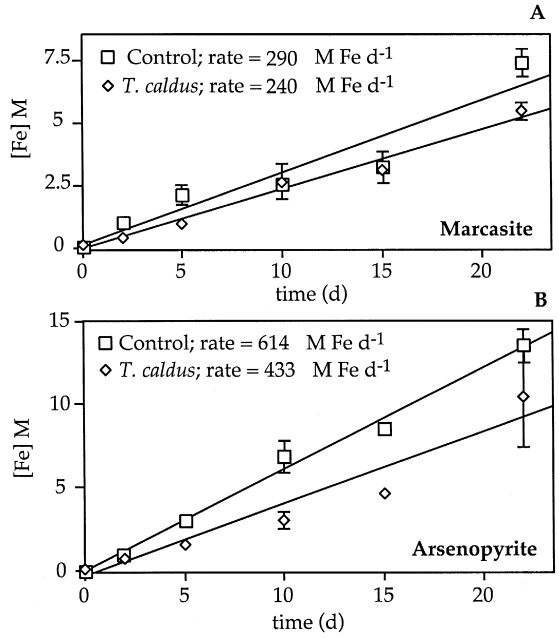

Fig. 5. Dissolution rate data for marcasite (A) and arsenopyrite (B). Data shown correspond with the same experiments for which Raman data are shown in Fig. 4. Data show iron release for samples reacted with *T. caldus* and abiotically in sulfuric acid (pH 1.5; modified after Edwards, 1999; Edwards et al., 1999c).

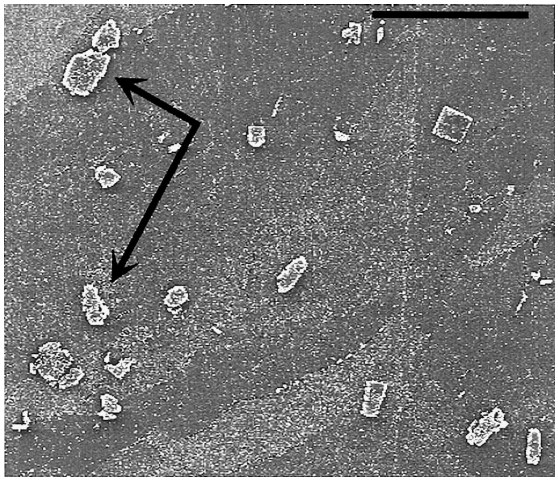

Fig. 6. The SEM image of sulfur-rich deposits on arsenopyrite, after abiotic reaction for 22 days at 37°C, pH = 1.5. Examples of sulfur-rich deposits (by EDX analysis; data not shown) are shown with arrows. Scale bar is 50 μm.

from the Raman data were effectively removing sulfur from the surfaces (Fig. 4). If sulfur were inhibiting dissolution, iron release rates would slow as sulfur accumulates at the surface. The fact that the dissolution rates in the presence of *T. caldus* were not higher than those of the abiotic control reactions suggests that either the sulfur layers are permeable to reactants and products of the surface reaction, or that the sulfur is not distributed uniformly across the surface. Indeed, some scanning electron microscopy images (Fig. 6) reveal agglomerates of sulfur present on the surface, surrounded by relatively "clean" areas. The ecological role of sulfur oxidizers, and why rates of sulfide dissolution are increased in mixed populations of iron- and sulfur oxidizers, remain poorly understood.

3. Biodiversity at Iron Mountain: seasonal and spatial relationships between microbial communities and geochemistry

Considerable prior attention has been given to the biology of drainage streams that deliver acidic, metal-rich waters from ore bodies or tailings piles to larger water ways. The microbial populations associated with these run-off environments are generally low in both biomass and diversity, and molecular analyses have suggested that most taxa in these environments are readily obtained via culturing techniques (Rawlings, 1995; Goebel and Stackebrandt, 1994b, 1995; Pizarro et al., 1996; Vasquez and Espejo, 1997). Our studies of run-off streams at Iron Mountain (Edwards et al., 1999a; Schrenk et al., 1998) are consistent with other studies that suggest that the dominant organisms detected are usually *T. ferrooxidans* and *L. ferrooxidans* (Rawlings et al., 1999; Walton and Johnson, 1992). However, our studies have also found that there is more that we can learn about the microbial diversity involved in sulfide dissolution by studying the microbial communities at subsurface sites (see below).

At Iron Mountain, as at other sites, the acidophilic community includes Eukarya, Bacteria and Archaea. At subsurface sites that receive no sunlight, chemosynthetic prokaryotes that utilize the reduced iron and/or sulfur from pyrite for energy and fix CO_2 for cell carbon are the foundation of the mine biota. Mixotrophic (assimilate organic or inorganic carbon as well as oxidize iron and/or sulfur) and heterotrophic (utilize organic carbon for energy) prokaryotes are often detected and play an important role in the ecology (Johnson, 1998). Filamentous fungi and protozoa are the most common eukaryotes observed (Schleper et al., 1995). Protozoa are typically found in biofilms, where they graze on bacterial cells within them (Fig. 7).

Because of the large number of studies that have identified *T. ferrooxidans* and *L. ferrooxidans* in AMD run-off environments, and the relative ease of culturing these bacteria, laboratory studies have concentrated on the role these two species play in sulfide dissolution. However, in the environment, diverse communities of acidophilic organisms may influence leaching rates and effect sulfide dissolution. Other species of both bacteria and archaea have been obtained from AMD environments, and a great deal has been learned by characterization of these. However, in order to assess the natural abundance of different species of microorganisms and thereby infer their relative importance to sulfide dissolution, it is difficult and usually inaccurate to enumerate organisms by culturing, and molecular methods are required for quantitative analysis. Molecular methods include fluorescent in situ hybridization (FISH) using oligonucleotide probes targeting ribosomal ri-

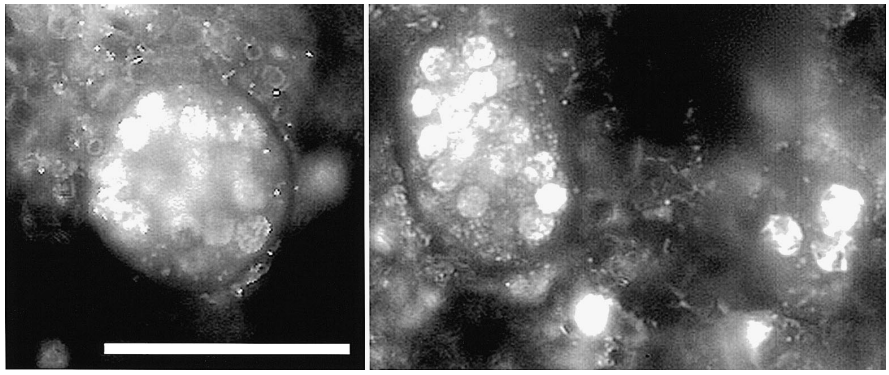

Fig. 7. DAPI-stained fluorescent image of protists within the subaerial biofilm that formed following a partial cave-in within the Richmond mine. Scale bar is 25 μm and applies to both images. Protist cells are large (10–20 μm diameter), roughly spherical, and contain many brightly fluorescent bodies, some of which contain ingested prokaryotes.

bonucleic acid (rRNA), and detection of ribosomal RNA gene sequences by polymerase chain reaction (PCR), cloning and sequence analysis (Amann et al., 1995; Pace et al., 1986).

The need for in situ molecular enumeration of biodiversity has been exemplified in many environments, AMD sites among others (e.g., Hugenholtz et al., 1998; Johnson, 1998, 1991; Amann et al., 1996; Goebel and Stackebrandt, 1994a,b; Barns et al., 1994). As one example, an early study at Iron Mountain tentatively identified *T. ferrooxidans* in drainage waters (Nordstrom, 2000). While this is consistent with more recent in situ molecular studies of run-off streams at Iron Mountain, it may tell us little about the microbial community at subsurface sites of primary acid generation. Studies using species-specific oligonucleotide probes to characterize populations from the Richmond Mine found that *T. ferrooxidans* rarely occurs at sites in contact with the ore body (Edwards et al., 1999a; Schrenk et al., 1998). In addition to problems with inferring microbial populations at acid-generating sites by studying run-off waters, the use of culturing techniques often selects an organism that can grow the fastest under the conditions provided, which may not reflect its natural abundance in the environment. For example, at the Richmond Mine, even when the abundance of *T. ferrooxidans* is below detection limit using FISH, the species can be cultured from the Richmond Mine using "9K" medium adjusted to pH 2.5 (unpublished data). While culturing techniques are vital for physiological assessment of microorganisms, these examples reinforce the importance of using quantitative, in situ molecular methods at primary sites of acid generation to identify key players involved in sulfide dissolution, in order to target and verify species of relevance.

3.1. Seasonal variations in microbial communities

Extensive analysis of samples from the Richmond Mine collected throughout 1 year indicated that substantial fluctuations in microbial community structure correlate with significant fluctuations in rainfall, ionic strength, and temperature (Fig. 8; Edwards et al., 1999a). Heavy rainfall in the winter is generally followed by summer droughts. Peaks and lows in discharge from the Richmond Mine correlate closely with precipitation, suggesting transit times for flow on the scale of days to a few weeks (P. Ekoniak, May 1999, personal communication). During times of low rainfall (summer droughts), the ionic strength of effluent is maximal.

Cell populations are found to be highest at the Richmond Mine during the dry summer and fall months. FISH indicates densities of 10^7–10^9 cells ml^{-1} total for bacteria, archaea and eukaryotes within sediments (pore fluids and attached to surfaces) from July through September (Edwards et al., 1999a). During the dry months, dense communities of microorganisms ($>10^9$ cells ml^{-1}), commonly referred to as slime streamers (see below), are also common. During the winter months, bacteria dominate the microbial population (Fig. 8). However,

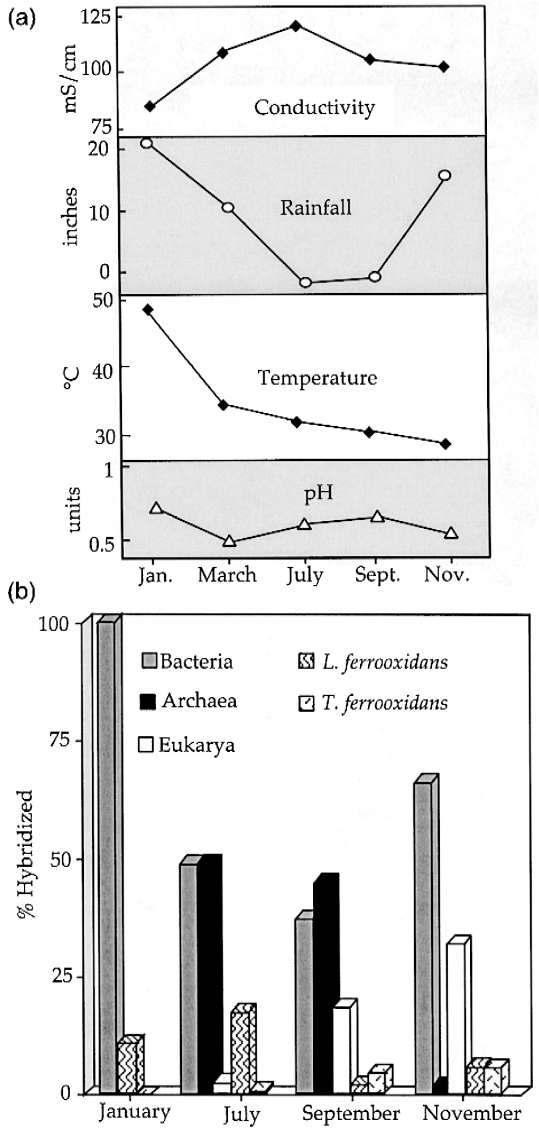

Fig. 8. Seasonal variations in environmental conditions and microbial populations at the Richmond Mine over 1 year (1997). (a) Conductivity, rainfall, pH, and temperature conditions. (b) Relative abundance of bacteria, archaea, eukarya, and the species, *L. ferrooxidans* and *T. ferrooxidans*. Microbial populations were quantitated using FISH (data from Edwards et al., 1999a).

during the summer and fall months, archaea represent a significant proportion of the microbial population. Correlations between high ionic strength and high archaeal numbers, and loss of archaea and dilution of solutions by rainfall, e.g., suggest probable geochemical controls on microbial community structure. However, analysis of the bacterial and archaeal impact on AMD generation requires metabolic analysis, and thus requires culturing and isolation of relevant species.

From enrichment cultures that were started with inoculum collected from the Richmond mine during the summer months when archaea are in high abundance, an iron-oxidizing archaea was isolated (fer1; Bond et al., 1999; Edwards, 2000). Analysis of 16*S* rRNA gene for fer1 indicates that the available sequence (849 bases) is identical to that of a recently described autotroph and bioleaching isolate, *F. acidophilum*. However, the archaea isolated from Iron Mountain are metabolically distinct. In comparison to *F. acidophilum*, fer1 has more extreme pH tolerance (grows well down to pH 0), higher temperature optimum (~45°C), and is capable of heterotrophic growth on yeast extract. Due to these physiological distinctions, the isolate has been tentatively given the species name *acidarmanus*, within the genus *Ferroplasma*. In situ analyses of the microbial community using species-specific probes for *F. acidarmanus* indicate that this archaea occurs in quite high abundance in the environment, comprising up to 85% of the total microbial community in some environments (Bond et al., 1999; Edwards, 2000). This species is inferred to be the archaea originally identified during the 1-year study (Edwards et al., 1999a). Given its predominance and widespread distribution, this iron-oxidizing species must play a significant role in AMD generation at Iron Mountain.

3.2. Population evolution over time: re-colonization events

Occasionally, periods of extremely heavy rainfall result in heavy washouts of the fine-grained pyrite sediments within the Richmond Mine. When this occurs, the sediments must be removed in order to provide access, and to keep the pipes that divert the acid waters from the mine clear of debris. One such occurrence (April 1998) provided an opportunity to study the evolution of the microbial population during re-colonization.

After the flow had subsided and the sediments removed in April 1998, very few microorganisms

were detectable on sediment surfaces or in sediment pore fluid ($< 10^4$ cells ml^{-1}), and slime streamers were washed away entirely. We attribute this to washout and removal of the microbially colonized upper sediment region (where there is sufficient oxygen diffusion to support growth). Shortly after this episode (July 1998), molecular analyses found that the majority of 16*S* rRNA gene sequences detected from sediment samples were from *Leptospirillum* Group II type, as represented by clone BU01 (Fig. 9). It has been suggested that *Leptospirillum* Group II types are the naturally abundant species (Goebel and Stackebrandt, 1995) and these may be the major types occurring in the mine. It is interesting to note that while these species accounted for $\leq 20\%$ of microbial populations associated with sediments during 1997 (Edwards et al., 1999b), they appear as the dominant initial colonizing species after this disturbance (unpublished data).

Re-colonization and return to the usual mine biota (slime streamers, etc.) associated with the sediments after this redistribution occurred only after a lengthy lag time ($\sim$ 4–6 months). FISH analyses of the microbial communities by November 1998 showed that *F. acidarmanus* dominated the microbial community, particularly in some slime streamers and sediments (Bond et al., 1999; Edwards, 2000). Cells hybridizing with a probe for *Leptospirillum* (Groups I + II) were detected in many samples, but these made up only low proportions of biofilms and sediments (unpublished data). One explanation is that the *Leptospirillum* dominating the 16*S* rRNA gene sequences detected in July 1998 decreased in abundance some months later and were succeeded by an abundance of *F. acidarmanus*. Hence, *F. acidarmanus* was a dominant second generation microbial constituent during re-colonization. Communities restructuring and changing geochemical conditions during re-colonization are undoubtedly coupled; hence, this sequence may only be applicable under the geochemical conditions that prevailed during this time. However, it seems probable that such reorganization occurs regularly following annual winter floods.

3.3. Taxonomic indications of redox gradients

Periodic slumps of pyritic material from overlying stoops are common events within subsurface tunnels at Iron Mountain. In November 1998, a slump developed from a partial cave-in of an above mine tunnel. Gelatinous material dripping from above formed a thick (up to 10 mm), subaerial biofilm on the slump surface. DAPI staining and molecular analysis indi-

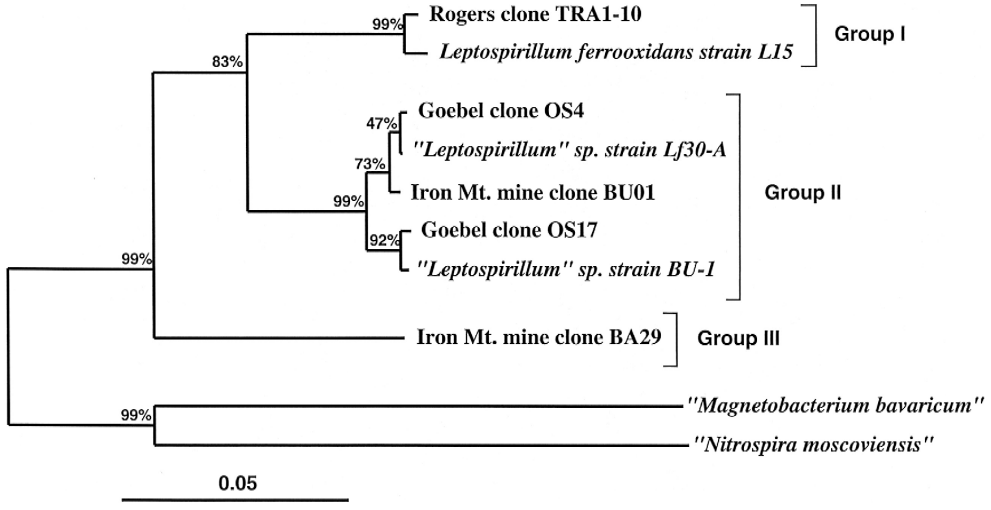

Fig. 9. Phylogenetic dendogram representing the evolutionary history of Iron Mountain mine clones with *Leptospirillum* species. This was inferred from comparison of DNA sequences, comprising 1163 nucleotides, of the 16*S* rRNA gene. Statistical confidence intervals of the tree topology are shown as bootstrap values at the branch points. Evolutionary distances are indicated by the sum of horizontal branch lengths; scale bar represents changes per nucleotide. Modified after Bond et al., in review.

cates the presence of novel diversity (Bond et al., in review). The major 16*S* rRNA gene sequence detected, represented by clone BA29 in Fig. 9, distantly (91% similar) related to *Leptospirillum* sequences, likely represents a new probable iron-oxidizing species or genus.

In addition to *Leptospirillum*, the subaerial biofilm contained organisms with sequences of varying similarity to cultured organisms of the *Acidimicrobium* group. Most of these were $>99\%$ similar to the recently described iron-oxidizing heterotroph, *Ferromicrobium acidophilus* (Bond et al., in review). Other sequences detected clustered within the delta subdivision of the *Proteobacteria* with low ($\sim 80\%$) similarity to these sequences. Detection of these sequences suggests that anaerobic respiration, sulfate or metal reduction may occur in the slime. It is likely that redox gradients and cycling of S and Fe compounds occur within the subaerial biofilm. To our knowledge, extremely acidophilic ($pH < 3$) sulfate-reducing species have not previously been described, although acid-tolerant, if not acidophilic sulfate reducers have been cultured in solutions down to pH 3 (B. Johnson, December 1999, personal communication).

3.4. Diversity at Iron Mountain: spatial considerations

Our analyses at Iron Mountain have found that limited types of organisms often dominate microbial communities in small-scale environments. This finding is consistent with that of other investigators who concluded that AMD communities are characterized by quite limited diversity (Goebel and Stackebrandt, 1995; Johnson, 1998). However, as can be seen from the above summary, the overall populations within the mine are quite diverse because the community structures change with time and space in response to changes in geochemical and physical conditions. As noted by Goebel and Stackebrandt (1994b, 1995), many of the previously identified organisms from these environments are cultivable and have been isolated. However, our recent molecular investigations indicate that novel 16*S* rRNA sequences and poorly studied species are present in extremely acidic environments. Development of new isolation procedures is required to obtain pure cultures for characterization of the novel organisms.

4. Kinetics of sulfide dissolution: evaluation of abiotic vs. microbial contributions to AMD

Microbial dissolution rates measured by numerous workers over several decades suggest considerable variability in the degree to which microorganisms accelerate oxidative dissolution (Olson, 1991). It is important to quantitatively measure microbially mediated dissolution rates under a variety of conditions in order to model AMD systems. However, the variability among microbial dissolution rates has made extrapolation to environmental settings difficult.

In order to better constrain microbial dissolution rates, Olson (1991) reported a comparison of leaching rates determined in eight different laboratories that all used the same strain of *T. ferrooxidans*, the same pyrite source, and the same leaching method (conditions, etc.). The results of these studies determined that *T. ferrooxidans* increased dissolution of pyrite relative to controls by an average of 34 times the abiotic rate (Olson, 1991). The important finding from this study was that microbial dissolution rates were fairly repeatable when experimental procedures and microbial strains were the same. However, even considering the consistency of these data, extrapolation to field settings is still problematic because two fundamentally crucial factors are often not considered: cell densities and surface area for reaction. First, cell densities are important because rates of pyrite dissolution are controlled by the rate of (microbial) re-oxidation of ferrous iron, which is necessarily linked to numbers of actively metabolizing cells. For the interlaboratory comparison, this was apparently not important, because enough parameters were constrained to ensure approximately comparable cell numbers in each experiment. However, environmental population sizes may differ dramatically from the optimized conditions used for laboratory experiments. Second, surface area is important because abiotic dissolution also contributes to the flux of iron and sulfur from pyrite surfaces, and these rates depend upon the surface area available for

reaction. Surface area is routinely determined for abiotic geochemical experiments, but not so often determined for microbial experiments. In sum, both cell number and surface area data are required for determination of rate constants that would allow extrapolation to the environment. Cell-normalized rate constants have been commonly determined for many microbially mediated processes, such as bacterial sulfate reduction (e.g., Kirsten and Canfield, 1997). In the case of sulfide oxidation, however, cell-normalized rates are not reported, due in part to the technical difficulties associated with accurately determining cell densities attached to sulfide particles.

In recent work, we determined cell-normalized dissolution rates for different mixed enrichment cultures and iron-oxidizing isolates that were obtained from the Richmond Mine (Edwards, 1999; Edwards et al., 1998, 1999b). Experiments were conducted under varying conditions of oxygenation, pH, and available surface area, type of sulfide mineral (pyrite, marcasite, arsenopyrite) and cell densities, so total dissolution rates varied considerably. However, cell-normalized dissolution rates clustered more tightly, from 2×10^{-8} to 6×10^{-7} μM Fe cell^{-1} day^{-1} (median $= 3 \times 10^{-7}$ μM Fe cell^{-1} day^{-1}). Thus, for order-of-magnitude environmental calculations, it may be possible to approximate the microbial contribution to dissolution by a constant. This is important because given information regarding two key environmental parameters, cell densities of iron-oxidizing microorganisms and surface area for reactions, the microbial contribution to sulfide dissolution can be estimated.

4.1. Application of cell-normalized dissolution rates to predict microbial contribution to AMD production

Cell-normalized dissolution rates provide the link necessary to make predictive estimates of the microbial contribution to AMD production in the environment. Here we briefly give an example of how this can be applied to a system such as the Richmond Mine at Iron Mountain. Although this is not intended to be a strictly quantitative analysis of AMD generation at Iron Mountain, it highlights where future analysis may be needed.

Fig. 10 shows a simplified diagram of the discharge system for the Richmond Tunnel System (Fig. 1). We will estimate the maximum microbial contribution to iron release into the Richmond mine effluent (Fig. 10), and approximate the amount of pyritic material that would need to react to produce the iron load coming from the Richmond Mine. These calculations are based on a recent measurement of iron concentrations in the Richmond effluent (~ 30 g l^{-1}; May 1998, unpublished data) and flow rate (~ 100 l min^{-1}; courtesy of Stauffer Management).

In Fig. 10, the mine tunnel environments are divided into two simplified "zones". Zone 1 consists of water flowing over pyrite sediments that are colonized by biofilms. Most of these biofilms exist as streamers in the water that are anchored within the sediments, rather than as a surface coating (Fig. 11). As noted above, the biofilms are comprised predominately of iron-oxidizing prokaryotes, although the particular species varies with time and space. Although the proportion of eukarya in biofilms varies, for these calculations, we will use the estimate from a recent study that determined eukarya to comprise $\sim 15\%$ of the volume of a biofilm (Bond et al., 1999; Edwards, 2000). We estimate that condensed biofilms are ~ 2 cm thick. Determining the prokaryotic cell density within biofilms is difficult because they are held within voluminous extracellular polymeric material that is not easily disaggregated without cell disruption. But if we estimate that each cell occupies ~ 8 μm^3 (using cubic geometry and estimating 2 μm diameter for each cell + extracellular material) and is closely packed, then $\sim 10^{11}$ prokaryotic cells can be accommodated in 1 cm^3 of biofilm. An upper estimate for the aerial extent of flowing water and biofilm material, based on and the need for flowing water to accommodate streamers and the estimated geometry of dendritic flow through the tunnels, is ~ 30 m^2, or $\sim 6 \times 10^3$ cm^3. At 10^{11} cells cm^{-3}, the biofilms contain $\sim 6 \times 10^{14}$ total cells. Hence, if we use the median cell-normalized dissolution rate of 3×10^{-13} M Fe cell^{-1} day^{-1}, the maximum contribution from the biofilms is ~ 200 M Fe day^{-1}, or $< 1\%$ of the 10^5 M of total iron output from the tunnel system (Fig. 10). Since this is a relatively minor contribution to the total iron flux, we will consider other sources, namely sediment

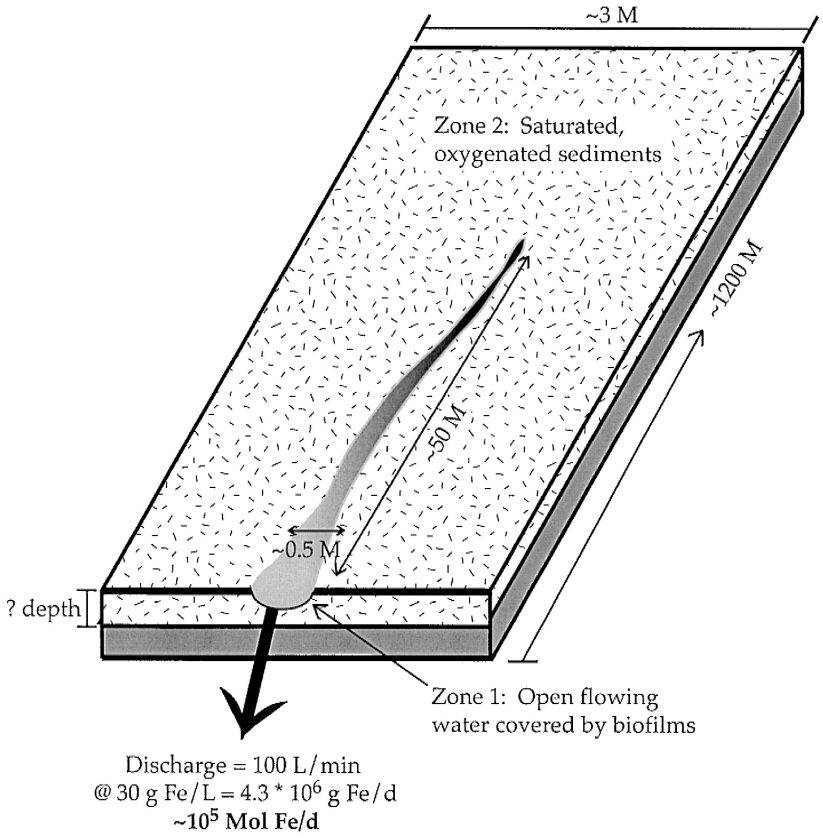

Fig. 10. Schematic diagram to represent a cross-section through the combined (length) Richmond Mine tunnels, that are shown in plan form in Fig. 1. The tunnel floors contain deep (> 1 m) accumulations of fine-grained pyrite sediments, which are represented as a wedge in the diagram. Some surface water flows in the tunnels, and is colonized by biofilms (Fig. 11). However, much of fluid flow within the tunnels is subsurface, resulting in loosely consolidated, saturated sediments. The depth of oxygen penetration is unknown; an oxygenated, saturated portion of the wedge (not scaled) is illustrated by the stippled pattern.

piles and the microbial cells associated with them, in the following calculations.

The remainder of the tunnel system consists of pyrite sediments at varying degrees of saturation and oxygenation. Much of the sediment is very loosely consolidated because subsurface water flows, which gives the tunnel floors a quicksand-like consistency in many areas. The surface area of the bulk sediments, which include some silicate materials, is highly variable. A measured value is $\sim 15 \times 10^{-2}$ $m^2\ g^{-1}$ (Edwards et al., 1998). This is comparable to the surface area used in laboratory experiments for determination of abiotic dissolution rates, at 2.3×10^{-2} $m^{-2}\ g^{-1}$, which was entirely sulfide material (Edwards, 1999; Edwards et al., 1999c). For the purposes of example calculations, we will use the rate determined in this study, 1.2×10^{-4} M Fe $cm^{-1}\ day^{-1}$ for the abiotic iron release rate.

To determine the microbial contribution to iron release, we need information on cell densities, and estimates of pore fluid space within the sediments. For these calculations, we will again be estimating an upper contribution to iron release by microorganisms. We estimate that 1 cm^3 of very loosely consolidated sediment contains ~ 2 g ($\sim$ 150–500 μm) of pyrite, which requires ~ 500 μl of solution to saturate pore space. The cell density of prokaryotes in sediments at the Richmond Mine (attached to surfaces and in pore fluids), as noted above, is maximal in the summer months, at $\sim 2 \times 10^9$ cells ml^{-1}

Fig. 11. Example of biofilms within the Richmond Mine. Stream width is ~1 m. Eukaryotic filaments are anchored within the underlying sediments and are colonized by iron-oxidizing prokaryotes, which comprise most of the biomass.

(Edwards et al., 1999a), or 10^9 cells cm^{-3}. At 10^9 cells cm^{-3}, using the cell normalized rate constant of 3×10^{-7} μM Fe $cell^{-1}$ day^{-1}, we obtain an upper estimate of the microbial contribution to dissolution within the sediments of 3×10^{-4} M Fe cm^{-1} day^{-1}. This calculation suggests that the abiotic and microbial contributions to iron release differ by less than the order of magnitude confidence we have for the calculation. This assessment contrasts laboratory measurements that indicate up to 34-fold increases in laboratory-determined microbial dissolution rates relative to controls (Olson, 1991; Paciorek et al., 1981). Moreover, these calculations suggest that the high rate of AMD generation at Iron Mountain may be largely due to the larger than anticipated inorganic contribution resulting from the high-surface area available for reaction. The temperature dependence of rates may also be a factor. Unlike the inorganic rate, the microbial rate seems to have a limited temperature dependence (Norris, 1990). Reactions within the Richmond Mine occur at ~20°C higher temperatures than those used in most laboratory studies, which may also explain the inferred greater contribution of inorganic dissolution at this site. Additionally, pore fluid constraints within saturated sediments will greatly reduce microbial population densities relative to most laboratory experiments. Population size will be pivotal to what the microbial contribution to dissolution in the environment can be.

Summing the abiotic and microbial contributions, we can estimate the release of iron from saturated, sufficiently oxygenated sediments to be ~4×10^{-4} M Fe day^{-1} cm^{-3}. Hence, if all of the iron in the effluent were coming from the tunnel sediments, ~250 m^3 of reacting sediment would be required to produce 10^5 M Fe day^{-1}. This volume of sediments is easily accommodated within the Richmond Mine (Figs. 1 and 10). However, it is difficult to estimate the depth to which pyrite dissolution occurs in the sediments because the rate of oxygen transport into sediments is poorly constrained. Determination of the mechanisms and rates of oxygen transport and diffusion has been previously recognized to be of first-order importance for assessing AMD production at Iron Mountain. Given the accessibility of pyrite accumulations in the tunnels to air and water, we emphasize the importance of explicit consideration of oxygen transport into saturated and semi-saturated sediments in future analyses.

Acknowledgements

D. Kirk Nordstrom is thanked for stimulating discussion. We also thank Iron Mountain Mine for site access and Stauffer Management for providing assistance. Support for this work was provided by NSF grant CHE-9521731.

References

Alpers, C.N., Nordstrom, D.K., Burchard, J.M., 1992. Compilation and interpretation of water quality and discharge for acidic waters at Iron Mountain, Shasta County, California. U.S. Geol. Surv. Bull., No. 91-4150.

Alpers, C.N., Nordstrom, D.K., Thompson, J.M., 1994. Environmental geochemistry of sulfide oxidation. In: Alpers, C.N., Blowes, D.W. (Eds.), American Chemical Society Symposium Series. American Chemical Society, Washington.

Amann, R.I., Ludwig, W., Schleifer, K., 1995. Phylogenetic identification and in situ detection of individual microbial cells without cultivation. Microbiol. Rev. 59, 143–169.

Amann, R., Snaidr, J., Wagner, M., Ludwig, W., Schleifer, K.H., 1996. In situ visualization of high genetic diversity in a natural microbial community. J. Bacteriol. 178, 3496–3500.

Barns, S.M., Fundyga, R.E., Jeffries, M.W., Pace, N.R., 1994. Remarkable archaeal diversity detected in a Yellowstone National Park hot spring environment. Proc. Natl. Acad. Sci. U. S. A. 91, 1609–1613.

Bhatti, T.B., Bigham, J.M., Carlson, L., Tuovinen, O.H., 1993. Mineral products of Pyrrhotite oxidation by *Thiobacillus ferrooxidans*. Appl. Environ. Microbiol. 59, 1984–1990.

Bond, P.L., Edwards, K.J., Gihring, T.M., Banfield, J.F., 1999. Microbial ecology of an acid mine drainage environment. Geological Society of America, 31st Annual Meeting. The Geological Society of America, Boulder.

Bond, P.L., Smriga, S.P., Banfield, J.F., in review. Phylogeny of microorganisms populating a thick, subaerial, predominantly lithotrophic biofilm at an extreme acid mine drainage site. In review.

Brown, A.D., Jurinak, J.J., 1989. Mechanism of pyrite oxidation in aqueous mixtures. J. Environ. Qual. 18, 545–550.

Curutchet, G., Tedesco, P., Donati, E., 1996. Combined degradation of covellite by *Thiobacillus thiooxidans* and *Thiobacillus ferrooxidans*. Biotechnol. Lett. 18, 1471–1476.

Dopson, M., Lindstrom, E.B., 1999. Potential role of *Thiobacillus caldus* in arsenopyrite bioleaching. Appl. Environ. Microbiol. 65, 36–40.

Edwards, K.J., 1999. The geomicrobiology of sulfide dissolution. PhD Thesis, University of Wisconsin, Madison, 311 pp.

Edwards, K.J., Schrenk, M.O., Banfield, J.F., Hamers, R.J., 1997. Oxidative dissolution of pyrite by microorganisms at Iron Mountain, California. The Geological Society of America, 29th Annual Meeting. The Geological Society of America, Boulder.

Edwards, K.J., Schrenk, M.O., Hamers, R., Banfield, J.F., 1998. Microbial oxidation of pyrite: experiments using microorganisms from an extreme acidic environment. Am. Mineral. 83, 1444–11453.

Edwards, K.J., Gihring, T.M., Banfield, J.F., 1999a. Seasonal variations in microbial populations and environmental conditions at an extreme acid mine drainage environment. Appl. Environ. Microbiol. 65, 3627–3632.

Edwards, K.J. et al., 1999b. Geomicrobiology of pyrite (FeS_2) dissolution: a case study at Iron Mountain. Calif. Geomicrobiol. J. 16, 155–179.

Edwards, K.J., McGuire, M.M., Hamers, R.J., Banfield, J.F., 1999c. Kinetics and surface microstructural evolution of microbially mediated sulfide dissolution: implications for modeling acid mine drainage generation. Ninth Annual V.M. Goldschmidt Conference. Lunar and Planetary Institute, Houston.

Edwards, K.J., Bond, P.L., Gihring, T.M., Banfield, J.F., 2000. An iron-oxidizing extreme acidophile important in acid mine drainage. Sci. 287, 1797–1799.

Fowler, T.A., Crundwell, F.K., 1999. Leaching of zinc sulfide by *Thiobacillus ferrooxidans*: bacterial oxidation of the sulfur product layer increases the rate of zinc sulfide dissolution at high concentrations of ferrous ions. Appl. Environ. Microbiol. 65, 5285–5292.

Garcia, O. Jr., Bigham Jerry, M., Olli, H., 1995a. Oxidation of galena by *Thiobacillus ferrooxidans* and *Thiobacillus thiooxidans*. Can. J. Microbiol. 41, 508–514.

Garcia, O. Jr., Bigham Jerry, M., Tuovinen Olli, H., 1995b. Sphalerite oxidation by *Thiobacillus ferrooxidans* and *Thiobacillus thiooxidans*. Can. J. Microbiol. 41, 578–584.

Garrels, R.M., Thompson, M.E., 1960. Oxidation of pyrite by iron sulfate solutions. Am. J. Sci. 259, 57–67.

Goebel, B.M., Stackebrandt, E., 1994a. The biotechnological importance of molecular biodiversity studies for metal bioleaching. In: Priest, F.G., Ramos-Cormenzana, A., Tindall, B.J. (Eds.), Bacterial Diversity and Systematics. Plenum.

Goebel, B.M., Stackebrandt, E., 1994b. Cultural and phylogenetic analysis of mixed microbial populations found in natural and commercial bioleaching environments. Appl. Environ. Microbiol. 60, 1614–1621.

Goebel, B.M., Stackebrandt, E., 1995. Molecular analysis of the microbial biodiversity in a natural acidic environment. In: Jerez, C.A., Vargas, T., Toledo, H., Wiertz, J.V. (Eds.), International Biohydrometallurgy Symposium IBS-95. University of Chile, Santiago, Chile, pp. 43–52.

Hugenholtz, P., Goebel, B.M., Pace, N.R., 1998. Impact of culture-independent studies on the emerging phylogenetic view of bacterial diversity. J. Bacteriol. 180, 4765–4775.

Johnson, D.B., 1991. Diversity of microbial life in highly acidic, mesophilic environments. In: Berthelin, J. (Ed.), Diversity of Environmental Biogeochemistry. Elsevier, Amsterdam.

Johnson, D.B., 1998. Biodiversity and ecology of acidophilic microorganisms. FEMS Microbiol. Ecol. 27, 307–317.

Kirsten, S.H., Canfield, D.E., 1997. Sulfur isotope fractionation during bacterial sulfate reduction in organic-rich sediments. Geochim. Cosmochim. Acta 61, 5351–5361.

Lowson, R.T., 1982. Aqueous oxidation of pyrite by molecular oxygen. Chem. Rev. 82, 461–497.

McGuire, M.M., Edwards, K.J., Banfield, J.F., Hamers, R.J., 1999. Formation of elemental sulfur on sulfide mineral surfaces. Geological Society of America, 31st Annual Meeting. The Geological Society of America, Boulder.

McGuire, M.M., Edwards, K.J., Banfield, J.F., Hamers, R.J., in review. Surface chemistry of sulfide minerals during microbially mediated oxidative dissolution.

McKibben, M.A., Barnes, H.L., 1986. Oxidation of pyrite in low temperature acidic solutions; rate laws and surface textures. Geochim. Cosmochim. Acta 50, 1509–1520.

Moses, C.O., Nordstrom, D.K., Herman, J.S., Mills, A.L., 1987. Aqueous pyrite oxidation by dissolved oxygen and by ferric iron. Geochim. Cosmochim. Acta 51, 1561–1572.

Nordstrom, D.K., 2000. Hydrogeochemical and microbiological factors affecting the heavy metal chemistry of an acid mine drainage system. PhD Thesis, Stanford University, Stanford, 230 pp.

Nordstrom, D.K., 1982. Aqueous pyrite oxidation and the consequent formation of secondary iron minerals. In: Kittrick, J.A., Fanning, D.S., Hossner, L.R., Kral, D.M., Hawkins, S. (Eds.), Acid Sulfate Weathering; Proceedings of a Symposium. Soil Science Society of America, Madison, pp. 37–56.

Nordstrom, D.K., Alpers, C.N., 1999a. Negative pH, efflorescent mineralogy, and consequences for environmental restoration at the Iron Mountain Superfund site, California. Proc. Natl. Acad. Sci. U. S. A. 96, 3455–3462.

Nordstrom, D.K., Alpers, N., 1999b. Geochemistry of acid mine waters. In: Plumlee, G., Logsdon, M. (Eds.), Reviews in Economic Geology. Society of Economic Geologists, Littleton, pp. 133–160.

Nordstrom, D.K., Southham, G., 1997. The geomicrobiology of acid mine drainage. Geomicrobiology: Interactions Between Microbes and Minerals. In: Banfield, J.F., Nealson, K.H. (Eds.), Reviews in Mineralogy Mineralogical Society of America, Washington, pp. 361–390.

Norris, P.R., 1990. Acidophilic bacteria and their activity in mineral sulfide oxidation. In: Erlich, H.L., Brierley, C. (Eds.), Microbial Mineral Recovery. McGraw-Hill, New York.

Olson, G.J., 1991. Rate of pyrite bioleaching by *Thiobacillus ferrooxidans*: results of an interlaboratory comparison. Appl. Environ. Microbiol. 57, 642–644.

Pace, R.N., Stahl, D.A., Lane, D.J., Olsen, G.J., 1986. The analysis of natural microbial population by ribosomal RNA sequences. Adv. Microbial. Ecol. 9, 1–55.

Paciorek, K.J.L., Kratzer, R.H., Kimble, P.F., Toben, W.A., Vatasescu, A.L., 1981. Degradation of massive pyrite: physical, chemical and bacterial effects. Geomicrobiol. J. 2, 363–374.

Pizarro, J., Jedlicki, E., Orellana, O., Romero, J., Espejo, R.T., 1996. Bacterial populations in samples of bioleached copper ore as revealed by analysis of DNA obtained before and after cultivation. Appl. Environ. Microbiol. 62, 1323–1328.

Rawlings, D.E., 1995. Restriction enzyme analysis of 16*S* rRNA genes for the rapid identification of *Thiobacillus ferrooxidans* and *Leptospirillum ferrooxidans* in leaching environments. In: Jerez, C.A., Vargas, T., Toledo, H., Wietz, J.V. (Eds.), Proceedings of the International Biohydrometallurgy Symposium IBS-95. University of Chile, Santiago, pp. 9–17.

Rawlings, D.E., Tributsch, H., Hansford, G.S., 1999. Reasons why "*Leptospirillum*"-like species rather *Thiobacillus ferrooxidans* are the dominant iron-oxidizing bacteria in many commercial processes for the biooxidation of pyrite and related ores. Microbiology 145, 5–13.

Rimstidt, D.E., Newcomb, W.D., 1992. Measurement and analysis of rate data: the rate of reaction of ferric iron with pyrite. Geochim. Cosmochim. Acta 57, 1919–1934.

Sasaki, K., Tsunekawa, M., Ohtsuka, T., Konno, H., 1995. Confirmation of a sulfur-rich layer on pyrite after oxidative dissolution by Fe(III) ions around pH 2. Geochim. Cosmochim. Acta 59, 3155–3158.

Schleper, C. et al., 1995. Picrophilus gen. nov., fam. nov.: a novel aerobic, heterotrophic, thermoacidophilic genus and family comprising archaea capable of growth around pH 0. J. Bacteriol. 177, 7050–7059.

Schrenk, M.O., Edwards, K.J., Goodman, R.M., Hamers, R.J., Banfield, J.F., 1998. Distribution of *Thiobacillus ferrooxidans* and *Leptospirillum ferrooxidans*: implications for generation of acid mine drainage. Science 279, 1519–1522.

Singer, P.C., Stumm, W., 1968. Kinetics of the oxidation of ferrous iron. Proceedings of the 2nd Symposium on Coal Mine Drainage Research. Bituminous Coal Research. National Coal Association, Pittsburg, pp. 12–34.

Singer, P.C., Stumm, W., 1970. Acidic mine drainage: the rate-determining step. Science 167, 1121–1123.

Stokes, H.N., 1901. On pyrite and marcasite. U.S. Geol. Surv. Bull., No. 186.

Vasquez, M., Espejo, R.T., 1997. Chemolithotropic bacteria in copper ores leached at high sulfuric acid concentrations. Appl. Environ. Microbiol. 63, 332–334.

Walton, K.C., Johnson, D.B., 1992. Microbiological and chemical characteristics of an acidic stream draining a disused copper mine. Environ. Pollut. 76, 169–175.

Wiersma, C.L., Rimstidt, J.D., 1984. Rates of reaction of pyrite and marcasite with ferric iron at pH 2. Geochim. Cosmochim. Acta 48, 85–92.

Williamson, M.A., Rimstidt, J.D., 1994. The kinetics and electrochemical rate-determining step of aqueous pyrite oxidation. Geochim. Cosmochim. Acta 58, 5443–5454.